Environmental Science Nano

ROYAL SOCIETY OF CHEMISTRY

PAPER

View Article Online
View Journal | View Issue

Cite this: *Environ. Sci.: Nano*, 2023, **10**, 129

Soil activity and microbial community response to nanometal oxides were not due exclusively to a particle size effect†

Helena Avila-Arias, [ab] Loring F. Nies,[c] Marianne Bischoff Gray,[a] Emiliano Barreto-Hernández [d] and Ronald F. Turco *[a]

Studies supporting assumptions that engineered nanomaterials (ENMs) are more toxic than their bulk counterparts are sparse. We have previously shown that soil response to ENM lithium oxide (nanoLi_2O) was not different than bulkLi_2O. Here we investigated how soil microbiota function responds to exposure to molybdenum oxide (MoO_3), nickel oxide (NiO), and zinc oxide (ZnO), either as bulk or the ENM equivalent, and to nanoLi_2O. We evaluated the solubility of bulk *vs.* ENM metal oxides and their influence on pH of saline solution and a nutritionally rich medium to understand their behavior in aqueous solution, as a simulation of soil pore water. Metal oxides more drastically affected pH of saline solution than aqueous media. Both forms of MoO_3 decreased soil acid phosphatase activity, pH, and total DNA. Soil exposure to highly soluble bulkMoO_3 showed an increase in bacterial and fungal biomass and relative abundance of *Acidobacteria*, *Nitrospira*, and *Proteobacteria*. Exposure to nanoMoO_3 increased prokaryotic alpha diversity. Both forms of relatively insoluble NiO decreased soil pH and microbial biomass. Both forms of ZnO (highly soluble in LB) increased soil pH while decreasing basal respiration and prokaryotic alpha diversity. BulkZnO decreased microbial biomass while nanoZnO decreased soil β-glucosidase and β-*N*-acetylglucosamidase activity and increased the relative abundance of *Firmicutes*. Soil exposure to nanoLi_2O showed the most significant change in soil pH (+2.83 units) and response. This study provides evidence that ENMs influenced soil function and microbial diversity and composition. However, we found no evidence that changes were caused exclusively by a nano-size effect.

Received 16th August 2022,
Accepted 21st November 2022

DOI: 10.1039/d2en00762b

rsc.li/es-nano

Environmental significance

Both chemical composition and morphological properties can impact nanomaterials' activity and behavior compared to their bulk counterpart. In this work, we address how nano and bulk forms of molybdenum-, nickel-, lithium-, and zinc oxide, and a nano form of lithium oxide affect soil function and the resident microbial communities. The type and potential concentration of released metal and the influence on soil pH appeared to be more of a substantial factor than the particles' size. Furthermore, we consider the effects of nano lithium oxide, which seemed to be driven by a rapid and drastic increase in soil pH, to be substantial and warrant significant concern. We suggest caution around the possible introduction of lithium oxide into the environment.

[a] *Department of Agronomy, College of Agriculture, Purdue University, 915 W. State Street, West Lafayette, IN, 47907, USA. E-mail: rturco@purdue.edu; Fax: +1 765 496 2926; Tel: +1 765 494 8077*
[b] *Ecological Sciences and Engineering Interdisciplinary Graduate Program, Purdue University, West Lafayette, IN, 47907, USA*
[c] *School of Civil Engineering and Environmental & Ecological Engineering, Purdue University, West Lafayette, Indiana 47907, USA*
[d] *Bioinformatics Group, Biotechnology Institute, Universidad Nacional de Colombia, Bogotá, Colombia*

† Electronic supplementary information (ESI) available: Extracellular enzymes assayed in soil exposed to metal oxides (Table S1); reactions to determine extracellular soil enzymes fluorometrically (Table S2); sequencing primers and thermocycler conditions for paired-end 16S rDNA V4/ITS1 community sequencing (Table S3); abundance of prokaryotic and fungal phyla in survey dataset (Table S4); metal oxide solubility (Fig. S1), soil enzyme activity (Fig. S2), pH, basal respiration, total DNA, biomass (Fig. S3 and S4), PLFAs (Fig. S5 and S6) in soils after exposure to metal oxides; differential abundance analysis of fungal (ITS1) phyla in soils exposed to metal oxides (Fig. S7); principal coordinate analysis depicting the quantitative Bray-Curtis distances of the 16S rDNA gene V4 and ITS1 sequences in soils after exposure to metal oxides (Fig. S8). See DOI: https://doi.org/10.1039/d2en00762b

Introduction

Nanotechnology represents high-growth scientific, engineering, and technology developments conducted at the nanoscale. Advancements in this field exploit novel properties of engineered nanomaterials (ENMs, materials with at least one dimension between 1–100 nm) in search of new materials and products and/or performance enhancements for existing products.[1] In this context, nanotechnology has been integrated into various disciplines, including agriculture, material science, electronics, and energy production. Exposure modeling studies show soils are expected to be the major sink of ENMs[2,3] entering the environment directly (as part of land application programs) or indirectly (released during all life cycle phases, *i.e.*, manufacturing, delivery, use, and/or disposal), thus becoming the next emerging category of contaminants.[4] Therefore, research on the current and potential nanotechnology-based solutions must include identifying harmful effects on soil caused by these materials. Soil is the foundation to plant, animal and human life[5] and harbors an exceptional diversity of microbes. One gram of soil contains billions of microbial cells with thousands of different genomes.[6,7] Soil microbes are key players in maintaining soil processes, *e.g.*, nutrient and gas recycling, degradation of organic materials, and maintaining ecosystem functions.[8,9] The introduction of anthropogenic materials such as ENMs may cause changes in soil microbial communities,[10] disturbing overall soil function and health, and the resilience of the ecosystem.[11] However, the effect and toxicity of different ENMs in soil are widely unknown.

Metal oxide ENMs, including molybdenum oxide (nanoMoO_3), nickel oxide (nanoNiO), and lithium oxide (nanoLi_2O), enable applications in a wide variety of advanced technologies, including batteries and fuel cells. Further, nanoMoO_3, nanoNiO, and nano zinc oxide (ZnO) are being investigated for their potential use as micronutrient nanofertilizers, and nanopesticides.[12–14] Previously, our research showed that nanoMoO_3, nanoNiO, and nanoLi_2O affected soil function.[15] Specifically, soil treated with nanoLi_2O at 474 μg Li g^{-1} released 3.45 times more CO_2 in comparison to the control. Additionally, β-glucosidase (BG) activity was decreased while urease activity increased following nanoLi_2O treatment. While no clear patterns were observed for CO_2, CH_4, and N_2O gas emissions in soils exposed to nanoMoO_3 and nanoNiO, we observed a temporary suppression of BG activity in soil treated with both metals. Bacterial, archaeal, and eukaryal microbial community structures were affected by increasing metal concentrations, except the archaea community was not affected by nanoLi_2O. This first effort to understand the toxicity of nanoMoO_3, nanoNiO, and nanoLi_2O led to more questions: i. is there a size (bulk *vs.* ENMs) effect on the toxicity of metal oxides?; ii. How do these metal oxides affect soil microbial biomass and diversity?; and iii. what microbial taxa in soil are affected by the metal oxides?

This work investigates how soil responds to chemical pollution with nanoLi_2O and ENM and bulk forms of MoO_3, NiO, and ZnO. We included nanoLi_2O to confirm earlier work on soil response but did not include its bulk form as our previous work had shown no difference between bulkLi_2O and nanoLi_2O.[15] We also evaluated the solubility of metal oxides and their influence on pH of saline solution and a nutritionally rich medium to understand their behavior in an aqueous solution, as in soil they will likely encounter soil pore water. In the soil, the variables that we measured included basal soil respiration (CO_2 emissions), enzyme activities involved in C, N, and P cycles (*i.e.*, β-glucosidases, *N*-acetylglucosaminidase, and acid phosphatase, respectively), microbial biomass (total DNA extracted, total phospholipids phosphate, and total fatty acid methyl esters), and community structure (fatty acid methyl ester) and diversity (16S rDNA gene V4 and ITS1 amplicon survey). Our prior work[15] suggested the effect of Li_2O was indirect due to a pH increase that was identified for either the bulk or nano form. ZnO was included as a positive control since it is known that Zn or ZnO affects microbial biomass,[16] decreases microbial community richness and diversity,[17–19] and affects enzymatic activity in soils.[18,19] The current study was focused on the first 14 days after metal oxide application because the most dramatic effects were previously observed within the first week of exposure.[15]

Materials and methods

Metal oxides

Size and purity of metal oxides used in this study are presented in Table 1. nanoLi_2O (Cat. NS6130-02-292), nanoMoO_3 (Cat. NS6130-03-333), and nanoNiO (Cat. NS6130-03-336) were purchased from Nanoshel® (Intelligent Materials Pvt. Ltd., Haryana, India), while nanoZnO (Cat. 30N-0801) was purchased from Inframat® (Advanced Materials TM LLC, Manchester, CT, USA). BulkMoO_3 (Cat. 203815), and bulkNiO (Cat. 481793) were purchased from Sigma-Aldrich, while bulkZnO (Cat. AA1113709) was purchased from Alfa Aesar (Tewksbury, MA, USA).

Solubility of metal oxides in aqueous media and pH determination

The solubility of metal oxides in aqueous media (0.9% saline solution (SS) and Luria-Bertani medium (LB)) was determined as this may be an essential property involved in toxicity. The pH change of aqueous media due to metal oxides was also determined at the end of the experiment (72 h). LB medium contained 10 g L^{-1} NaCl, 10 g L^{-1} tryptone, and 5 g L^{-1} yeast extract. Experiments were done in triplicate, including a set of controls, *i.e.*, only aqueous media without metal oxide addition. Metal oxides (25 mg) were added to 1 L sterile glass bottles and sterilized by incubating at 65 °C for 24 h. Upon sterilization, sterile lids were placed, and bottles were transferred to a sterile laminar flow cabinet and allowed to reach room temperature. Aqueous media (500 mL) were

Table 1 Metal oxides and single dose concentrations added to soil microcosms in this study

Compound	Size reported[a] (nm)	Size confirmation[b] (nm)	Purity[a] (%)	Vendor	Actual metal oxide[c,d] (μg g_{dw} per soil)	Calculated metal[e] (μg g_{dw} per soil)
NanoLi_2O	80–100	41.4 ± 10.2	99.9	Nanoshel	1070.6 ± 7.8	497.3 ± 3.6
BulkMoO_3		755.6 ± 255.6	99.97	Sigma-Aldrich	260.2 ± 1.0	173.4 ± 0.7
NanoMoO_3	<80	63.9 ± 16.9	99.9	Nanoshel	254.2 ± 3.0	169.4 ± 2.0
BulkNiO		186.4 ± 69.8	99.995	Sigma-Aldrich	1195.9 ± 2.1	939.8 ± 1.6
NanoNiO	<80	45.0 ± 10.1	99+	Nanoshel	1192.8 ± 1.5	937.4 ± 1.2
BulkZnO		222.0 ± 109.9	99.999	Alfa Aesar	498.6 ± 1.3	400.5 ± 1.0
NanoZnO	30	27.9 ± 9.4	99.7+	Inframat	498.9 ± 0.9	400.8 ± 0.7

[a] According to certificate of analysis from vendor. [b] Confirmation using Scanning Electron Microscope (SEM) at the Life Science Microscopy Facility at Purdue University, West Lafayette, IN, USA. $n \geq 50$. [c] Calculation based on the actual amount of metal oxide added to each soil microcosm (350 g dry weight equivalent (g_{dw}) soil). [d] Average ±standard deviation, $n = 3$ microcosms. [e] Calculated metal concentration in microcosms based on molar equivalence of the actual added metal oxide.

added to reach a final concentration of 50 μg mL^{-1} of metal oxide (MoO_3, NiO, ZnO). The suspensions were sonicated in a sonication bath (Heat Systems-Ultrasonics Inc., Plainview, New York) for 20 min and then transferred to an orbital shaker (150 rpm) and maintained at 25 °C for 72 h. Samples (10 mL) for metal determination were taken using a 10 mL pipette at 0, 6, 12, 24, 48, and 72 h after sonication. For metal determination, samples were centrifuged at 10 000*g* for 30 minutes, and the supernatants were separated and filtered through a 0.22 μm mixed cellulose ester membrane.[20] Dissolved metal concentration in the filtrate was determined using inductively coupled plasma mass spectrometry after diluting the samples (1/10) in 1% HNO_3. Detection/quantification limits were 1.3/9.8, 0.6/9.5, and 7.5/10.5 μg L^{-1} of Ni, Mo, and Zn, respectively, which allow reporting metal dissolution >0.2% after correcting for background metal content. Background metal content in saline solution for Ni and Mo were below detection limits (BDL), while Zn was below quantification limits (BQL). Background metal content in LB medium for Ni was BDL, for Mo was BQL, and for Zn was 0.812 ± 0.009 μg mL^{-1}.

Samples (10 mL) for pH measurement were taken using a 10 mL pipette at the end of the experiment (72 h) and determined using a glass electrode.

Soil microcosms

To understand the toxicity of ENM and bulk form of metal oxides (MoO_3, NiO, and ZnO) and nanoLi_2O on soil microbial communities and function, ENM or bulk metal oxide were applied at single concentrations shown by previous research to have an effect in soil bacterial communities (Table 1).[15–18]

Soil from a corn/soybean rotation field (0–10 cm) was collected from the Agronomy Center for Research and Education (ACRE), Purdue University, West Lafayette, IN, USA (40°29′56.7″N 86°59′51.5″W). This Drummer soil (Fine-silty, mixed, superactive, mesic Typic Endoaquolls) had a silty clay loam texture (20% sand, 50% silt, and 30% clay). It contained 3.5% organic matter and a cation exchange capacity (CEC) of 17.0 milliequivalents per 100 g of soil. All visible plant tissues, fauna, and other debris were removed, and soil was sieved (2 mm) and stored in the dark at room temperature before use.

Microcosms comprised 350 g dry weight equivalent (g_{dw}) soil in 1 L mason jars. Metal oxides were added at single doses (Table 1) directly to the soil in powder form, mixed thoroughly, and water content was adjusted to −0.03 MPa of water holding capacity. After the ENM or bulk metal oxide addition (considered as day 0), microcosms were covered using plastic covers with four 1 inch perforations to allow for air exchange and incubated in the dark at 21 °C for 15 days. Soil water content was monitored by measuring gravimetric water loss and maintained at 0.03 MPa. Soil samples were collected on days 1, 7, and 14. The experimental variables analyzed to monitor soil microbial biomass, diversity, composition, and function included basal soil respiration, soil enzymes (β-glucosidase, β-1,4-*N*-acetylglucosaminidase, and acid phosphatase), pH (glass electrode, 1 : 2, soil : water ratio), microbial biomass (phospholipid-phosphate, PL-PO4), microbial community structure (fatty acid methyl esters or FAMEs), total DNA, and prokaryotic and fungal diversity (16S rDNA gene V4 /ITS1 metagenomic survey). All treatments were replicated three times, including the no metal controls.

Soil basal respiration

Carbon dioxide (CO_2) concentration was determined by gas chromatography using the method described previously.[15] Briefly, microcosms were flushed with air for 2 min, and a gas-tight sampling lid was placed atop the jar using aluminum canning rings. Gas-tight sampling lids consisted of standard canning lids pierced with a preassembled rubber septum port to allow for sampling. Four 25 mL headspace gas samples were collected at hours 0, 1, and 2, using a 30 mL hypodermic Luer-lock syringe. Gas samples were transferred to 20 mL GC vials (Agilent, Santa Clara, CA, USA catalog # 5188-2753) previously evacuated to $<10^{-5}$ MPa and sealed with magnetic caps (Agilent, Santa Clara, CA, USA catalog # 5188-2759). Gas concentrations were determined by gas chromatography using external standards (Matheson Tri-gas, Montgomery, PA, USA). Gas emissions were expressed on a mass basis by using the universal gas law, accounting for

microcosm headspace volume, temperature, and atmospheric pressure, and then normalized to dry soil weight equivalent. Gas values were used to fit a regression line and slopes (gas emission rates, as μg CO_2–C g_{dw}^{-1} h^{-1}) per microcosm were used for further statistical analysis.

Extracellular enzyme activity assays

Enzyme assays were determined in soil samples obtained on 1, 7, and 14 d of the experiment and began within 2 h of sample collection. The activities of three hydrolytic enzymes (Table S1†) involved in carbon (β-1,4-glucosidase, BG, EC 3.2.1.21), nitrogen (β-1,4-*N*-acetylglucosaminidase, NAG, EC 3.1.6.1) and phosphorous (acid phosphatase, AP, EC 3.1.3.2) turnover were measured according to the protocol of Saiya-Cork *et al.*, 2002.[21] The determinations were performed using 96-well microplates, with eight replicate wells per sample per assay, including eight replicate wells for each blank, negative control, and quench standard (Table S2†). Fluorescence was measured on a fluorescent microplate reader (Wallac VICTOR 3 V 1420 Multilabel Counter; Perkin Elmer Life Sciences, Waltham, MA, USA) with 365 nm excitation and 450 nm emission filters. After correcting for controls and quenching, the activity of the soil enzymes was expressed on a soil dry weight and given in units of nmol h^{-1} g^{-1}.

Phospholipid-phosphate ($PL\text{-}PO_4$) and fatty acid methyl ester (FAME) analysis

The samples' microbial biomass and soil microbial community structure were estimated using $PL\text{-}PO_4$ and FAME profiles, respectively. Analytical recovery for the procedure was determined by adding phospholipid 17:0 (1,2-diheptadecanoyl-*sn-glycero*-3-phosphoethanolamine, Avanti Polar Lipids, Alabaster, AL, USA) as an extraction standard. Blanks consisting of tubes with extraction standards were extracted along with the samples to identify potential contamination. All solvents and chemicals used were of GC-analytical grade. All glassware was baked at 400 °C >4 h to remove lipid contaminants. Soil lipids were extracted from 5 g lyophilized soil subsamples following the method previously described,[22,23] and modified.[24] Briefly, lipid-soluble components were extracted from the soil with a single-phase mixture (1 : 2 : 0.8 v/v/v) of chloroform, methanol, and phosphate buffer. The chloroform layer was extracted and concentrated by evaporation under N_2. Total lipid extracts were resuspended in chloroform and transferred to a silicic acid column where phospholipids were separated from other lipids (*i.e.*, neutral and glycolipids) using a series of solvents of increasing polarity (*i.e.*, chloroform and acetone) and eluted with methanol into a clean vial. At this point, 10% of the phospholipid extract was used to estimate total biomass after potassium persulfate digestion using a colorimetric assay.[23] The remaining 90% of the extract was used to characterize community structure. The phospholipid extract was converted to FAMEs by mild alkaline methanolysis.[25] C19:0 (methyl nonadecanoate N5377, Sigma Aldrich, St. Louis, MO, USA) was added to all FAME samples as an internal standard. FAMEs were separated on a capillary gas chromatograph using an Agilent 7890 GC equipped with a capillary column (Rt-2560, 100 m, 0.25 mm ID, 0.20 μm df, Restek Corporation, Bellefonte, PA, USA) and identified by mass spectrometry with an Agilent 5975 mass spectrometer detector (Agilent, Santa Clara, CA, USA). Compounds in samples were quantified based on the area under the chromatogram peak in comparison with the standards (Supelco 37-component FAME mix, Sigma-Aldrich, St. Louis, MO, USA) and using the C19:0 internal standard.

A total of 21 different FAMEs were identified and quantified. Fatty acid nomenclature was used as previously described.[22] FAMEs were grouped based on their structure: straight-chain saturated fatty acids (14:0, 15:0, 16:0, 18:0), methyl-branched fatty acids (10-Me16:0, 10-Me18:0), monounsaturated fatty acids (14:1w5, 16:1w7c, 16:1w, 18:1w9c, 18:1w), cyclopropyl saturated fatty acids (cy17:0, cy19:0), terminally branched fatty acids (i14:0, i15:0, a15:0, i16:0, i17:0, a17:0), and polyunsaturated fatty acids (18:2w6t, 18:2w6c). Straight-chain saturated fatty acids were associated with bacteria. Saturated PLFAs were used as a biomarker for Gram-positive bacteria (*i.e.*, methyl-branched fatty acids and terminally branched saturated fatty acids). Methyl-branched fatty acids were used as a biomarker for actinomycetes. Monounsaturated fatty acids and cyclopropyl saturated fatty acids were used as biomarkers for Gram-negative bacteria. Polyunsaturated fatty acid 18:2w6c was used as a biomarker for fungi.[26–29] Ratios of fungal to bacterial biomass (F : B) were calculated by dividing the sum of 18:1w9c and 18:2w6c by the sum of FAMEs associated with bacteria.[26,30]

The $PL\text{-}PO_4$ and FAME signatures were expressed as the absolute abundance (nmol g $soil^{-1}$) and by the proportional abundance (mol%).

Soil DNA extraction and quantification

Genomic DNA was extracted from 0.75 g of soil using the PowerSoil® DNA Isolation kit (MO BIO Laboratories, Carlsbad, CA, USA) following the manufacturer's instructions. Since the DNA extraction kit manufacturer suggests 0.25 g of sample size, DNA was extracted from three 0.25 g portions of each microcosm, and extracts were pooled. DNA quality was assessed visually by electrophoresis on agarose gel (1%). DNA quality was also determined using NanoDrop 2000 UV-vis Spectrophotometer (Thermo Fisher Scientific Inc., Wilmington, DE, USA), based on the absorbance ratios of 260/280 nm (*i.e.*, an indicator of purity from protein contamination, which should be around 1.8–2.0) and of 260/230 nm (*i.e.*, DNA purity from contaminants such as phenol or chaotropic salts, >1.7). Total DNA quantification was done using the Qubit® dsDNA BR Quantification Assay Kit and a Qubit® 2.0 Fluorometer (Life Technologies, Foster City, CA, USA). The DNA extracted was stored at −20 °C until use.

16S rDNA gene V4 and ITS1 metagenomic survey

PCR amplification was performed at the Biosciences Division (BIO) Environmental Sample Preparation and Sequencing Facility (ESPSF) at Argonne National Laboratory (Lemont, IL, USA), as previously described[31,32] and following the Illumina amplification protocols from the Earth Microbiome Project for the 16S rDNA gene (**http://press.igsb.anl.gov/earthmicrobiome/emp-standard-protocols/16s/**) and ITS1 (**http://press.igsb.anl.gov/earthmicrobiome/protocols-and-standards/its/**). Briefly, DNA samples were diluted to 2.5 ng μL^{-1} for PCR amplification of the 16S rDNA gene variable region 4 (V4) and the internal transcribed spacer region 1 (ITS1) using primer sets 515f/806r and ITS1f/ITS2, respectively (Table S3†). A total of 25 μl PCR reaction mixture consisted of Platinum Hot Start PCR Master Mix (0.8X) (cat. no. 13000014, ThermoFisher), each of the primers (0.2 μM), and 1 μl of genomic DNA. Triplicate PCR reactions were performed for each sample, and PCR products were pooled at equimolar concentrations and purified using the UltraClean PCR clean-up kit (MO BIO Laboratories, Carlsbad, CA, USA). Pooled purified PCR product (30 ng) from each of the three replicate PCR reactions were combined into a single pool for Illumina MiSeq sequencing at the BIO ESPSF.

16S rDNA gene V4 analysis was conducted using pared-end reads, while only forward reads (higher quality) were used for ITS analysis. Raw Illumina fastq reads were processed through Trimmomatic[33] v0.39 to remove the adapter and obtain high-quality clean reads. High-quality reads were then analyzed using the Quantitative Insights Into Microbial Ecology 2 (QIIME2)[34] v2020.11. After high-quality reads were demultiplexed, DADA2 algorithm[35] was used for sequence quality control, including denoising, dereplication, and filtering of chimeras. To further reduce sequencing errors, amplicon sequence variants (ASVs) retained were observed in at least two samples, assigned at least to a phylum taxonomic level, and did not match mitochondria or chloroplast. Q2-diversity QIIME2 plugin was used for α- and β-diversity analysis and statistics of filtered rarefied feature tables. For sample comparison, libraries were rarefied to a common minimum number of sequences. Taxonomical assignment of ASVs was performed by BLASTing the representative sequences against customized Scikit-learn[36] trained on 16S rDNA gene V4 (515F/806R) and ITS1 within the SILVA[37–39] v138 at 99% similarity and UNITE[40] v8.2 at 97% similarity, respectively.

The α-diversity (*i.e.*, within sample diversity) was estimated by the number of observed ASVs (richness), evenness (Pielou's evenness), Faith's phylogenetic diversity and Shannon's diversity index. The β-diversity (*i.e.*, between sample diversity) metrics, Jaccard, Bray-Curtis, unweighted UniFrac, and weighted UniFrac distances, were calculated in QIIME2 using the q2-diversity plugin. The impact of metal oxides on soil α-diversity was determined using the Kruskal–Wallis rank sum test (non-parametric, one-way ANOVA), while the differences in β diversity indexes were tested using non-parametric multivariate analysis of variance (permutational MANOVA) with 999 permutations. EMPeror[41] tool was also used for visualizing 3D Principal Coordinate Analysis (PCoA) community data. To detect differences in the relative abundance of taxa between treatments (control *vs.* treatment or bulk *vs.* ENM), differential abundance analysis was performed using DESeq2 (ref. 42) in the MicrobiomeAnalyst[43,44] platform.

16S rDNA gene V4 and ITS1 marker gene survey raw data were deposited at the National Center for Biotechnology Information under the BioProject PRJNA813154. Data can be accessed using the following reviewer link: **https://dataview.ncbi.nlm.nih.gov/object/PRJNA813154?reviewer=776058mcjhen54ekeicj9e7kkq** and will be publicly available upon peer-reviewed publication.

Statistical analysis

All statistical analyses were performed with the software package SAS v9.4 (SAS Institute Inc., Cary, NC, USA). The univariate procedure (PROC UNIVARIATE) in SAS was used to evaluate statistical assumptions (univariate normality and homogeneity of variance) prior to analysis of variance. Raw data was used for statistical analysis, except for enzyme and pH data which were transformed ($\ln(x + 1)$ and $1/x$, respectively) to fulfill assumptions. In all cases, two-way ANOVA was used to examine statistical differences by treatment and sampling day and interaction between variables. Post-hoc Dunnett's test was used to assess treatment *vs.* control and size (bulk *vs.* ENM) main effects while Tukey–Kramer's test was used to compare day and treatment effects. Statistically significant differences were identified as $p < 0.05$, while highly statistically significant differences were identified as $p < 0.0001$. Logarithm (base 10) of the relative response (*i.e.*, soil response to metal oxide/response of soil control) was used to illustrate the reaction of metal oxides, where positive and negative numbers represent an increase or decrease in activity, respectively. Graphs were made using SigmaPlot v13.0 (Systat Software, San Jose, CA, USA).

Results

Metal oxide dissolution and pH in aqueous media

Metal oxide solubility was evaluated in 0.9% saline solution (SS) and LB medium (Table 2). BulkMoO_3, and ZnO (both bulk and ENM) reached a dissolution equilibrium after ~1 day in solution (Fig. S1†). At an initial concentration of 50 μg mL^{-1} of metal oxide, BulkMoO_3 was more soluble in SS (89.7 ± 0.5%) than in LB (68.3 ± 1.4%), while both bulk and nanoZnO were more soluble in LB (95.7 ± 0.7% and 96.2 ± 4.3%, respectively). NanoNiO was slightly soluble (<2%) in both aqueous media, while nanoMoO_3 and bulkNiO were not soluble in either SS nor LB.

Media pH was determined at the end of the dissolution experiment (Table 2). The pH of the control saline solution (no metal oxide added) was affected by all metal oxides;

Table 2 Dissolved metal oxide and pH of aqueous media after 72 h of dissolution of nano- or bulk metal oxide (50 μg mL^{-1}, as metal oxide). Average ±1 standard deviation are presented (n = 3). An asterisk represents significant difference ($p < 0.05$) in pH between treatments (metal oxide *vs.* control) or sizes (bulk *vs.* ENM) within metal oxide

	0.9% saline solution						LB medium					
	Dissolved metal oxide[a] (%)		pH		Treatment[b]	Size[c]	Dissolved metal oxide[a] (%)		pH		Treatment[b]	Size[c]
Control			5.35	±0.08					6.83	±0.01		
$BulkMoO_3$	89.7	±0.5	3.64	±0.07	*	*	68.3	±1.4	6.84	±0.03		*
$NanoMoO_3$	BQL[d]		4.78	±0.01	*		BQL		6.97	±0.01	*	
BulkNiO	BQL		6.21	±0.38	*		BQL		6.95	±0.01	*	
NanoNiO	1.3	±0.5	6.19	±0.13	*		0.9	±0.2	6.97	±0.01	*	
BulkZnO	7.9	±0.2	7.48	±0.06	*		95.7	±0.7	7.06	±0.00	*	
NanoZnO	9.6	±1.2	7.37	±0.12	*		96.2	±4.3	7.04	±0.01	*	

[a] Dissolved metal oxide (%) calculated using the concentration of dissolved metal (as determined by inductively coupled plasma mass spectrometry), the molar fraction of metal in metal oxide, and the percentage of calculated metal oxide dissolved out of the initial added concentration of 50 μg of metal oxide mL^{-1}, *e.g.*, $29.9\ \mu g\ Mo\ mL^{-1} \times \frac{1\ \mu mol\ Mo\ mL^{-1}}{95.95\ \mu g\ Mo\ mL^{-1}} \times \frac{1\ \mu mol\ MoO_3\ mL^{-1}}{1\ \mu mol\ Mo\ mL^{-1}} \times \frac{143.95\ \mu g\ MoO_3\ mL^{-1}}{1\ \mu mol\ MoO_3\ mL^{-1}} \times \frac{100\%}{50\ \mu g\ MoO_3\ mL^{-1}} = 89.7\%$. [b] Treatment column refers to statistical difference ($p < 0.05$) in pH between soils untreated (control soils, no metal oxide addition) and treated with metal oxide. [c] Size column refers to statistical difference ($p < 0.05$) in pH between soils treated with bulk- and nano-sized metal oxide. [d] BQL = Below quantification limit.

Table 3 Soil response to metal oxide addition. Treatment effects were determined by two-way ANOVA performed on raw or transformed (ln(x + 1) for enzyme activity and 1/x for pH) data. Post-hoc Dunnett's test was used to assess metal oxide (control *vs.* treatment) and size (bulk *vs.* ENM) effects

	Enzyme activity[a]								Basal respiration		Total DNA		Microbial biomass	
	AP[b]		BG[c]		NAG[d]		pH		μg CO_2–C g_{dw}^{-1}		nmol DNA g_{dw}^{-1}		nmol PL-PO_4 g_{dw}^{-1}	
	% change	p	% change	p	% change	p	Unit change	p	% change	p	% change	p	% change	p
Control *vs.*														
$NanoLi_2O$	−8.6	<0.001	−14.0	0.007	−5.5	0.024	2.83	<0.001	119.3	<0.001	−22.5	<0.001	29.0	0.054
$BulkMoO_3$	−14.3	<0.001	8.2	0.163	1.3	0.844	−0.19	0.003	27.5	0.300	−13.6	0.018	21.4	0.182
$NanoMoO_3$	−20.7	<0.001	9.9	0.057	−2.3	0.442	−0.13	0.054	30.9	0.238	−13.8	0.016	−14.9	0.462
BulkNiO	2.3	0.469	8.8	0.418	−0.8	0.977	−0.11	0.007	−3.9	0.692	−11.4	0.074	−27.9	0.022
NanoNiO	−0.1	1.000	10.7	0.252	1.6	0.828	−0.14	<0.001	0.4	0.968	−3.2	0.915	−9.1	0.745
BulkZnO	−1.9	0.650	11.1	0.222	−3.2	0.326	0.20	<0.001	−24.5	0.012	−4.7	0.788	−5.3	0.953
NanoZnO	1.6	0.751	18.4	0.013	−5.5	0.031	0.22	<0.001	−27.4	0.004	12.4	0.049	24.0	0.052
Bulk *vs.* ENM														
MoO_3	8.1	<0.001	−1.5	0.721	3.7	0.049	−0.06	0.692	−2.6	0.698	0.3	0.945	42.6	0.006
NiO	2.4	0.227	−1.8	0.582	−2.4	0.093	0.04	0.593	−4.3	0.657	−8.5	0.107	−20.6	0.050
ZnO	−3.4	0.074	−6.2	0.407	2.4	0.375	−0.01	0.988	4.0	0.756	−15.2	0.004	−23.6	0.019

[a] nmol h^{-1} g_{dw}^{-1}. [b] AP: acid phosphatase. [c] BG: β-glucosidase (BG). [d] NAG: β-*N*-Acetylglucosamidase.

MoO_3 decreased pH, while NiO and ZnO increased it. $BulkMoO_3$ decreased saline solution pH by 1.71 units, while $nanoMoO_3$ decreased it by 0.57 units. There was no difference between bulk and ENM for NiO (p = 1.0) and ZnO (p = 0.9716). In the control LB medium (no metal oxide added), metal oxides increased pH significantly ($p < 0.0001$), except $bulkMoO_3$. The pH increase was around 0.14, 0.13, and 0.22 units for $nanoMoO_3$, NiO and ZnO.

Soil enzymes

Acid phospatase (AP), β-glucosidases (BG), and *N*-acetylglucosaminidase (NAG) were used to evaluate metal oxide effect on phosphorous, carbon, and nitrogen cycles, respectively. Overall, $nanoLi_2O$, $bulkMoO_3$, and $nanoMoO_3$ significantly decreased AP activity 9%, 14%, and 21%, respectively (Table 3). Neither form of NiO or ZnO affected soil AP activity. $NanoLi_2O$ and MoO_3 effects on soil AP activity were observed 1, 7, and 14 days after metal oxide application (Fig. S2†). Soil BG activity was significantly decreased (14%) by $nanoLi_2O$ while significantly increased (18%) by nanoZnO. Interaction of treatment by day was not observed. Likewise, soil NAG activity was significantly decreased by $nanoLi_2O$ (5.5%) and nanoZnO (5.5%). Soil NAG responded significantly differently to $bulkMoO_3$ and $nanoMoO_3$, with a 4% higher response by the bulk counterpart. Interaction of treatment by day was not observed.

Soil pH

Soil pH was significantly increased by nanoLi_2O (2.83 units), bulkZnO (0.20 units), and nanoZnO (0.22 units) (Table 3). Soil pH was decreased by bulkMoO_3 (0.19 units), bulkNiO (0.11 units), and nanoNiO (0.14 units).

The interaction effect (treatment *vs.* day) on soil pH was significant (Fig. S3A†). NanoLi_2O and nanoZnO increased soil pH during the length of the experiment (14 days), while soils exposed to bulkMoO_3 and bulkZnO recovered to their original pH by the end of the experiment. NanoMoO_3 nor NiO (bulk or ENM) did not affect soil pH on specific sampling days. Also, there was no difference in the response between the bulk and ENM forms of the metal oxides.

Soil basal respiration

NanoLi_2O significantly increased (119%) soil basal respiration (Table 3), which continued during the length of the experiment (Fig. S3B†). Neither MoO_3 nor NiO affected soil basal respiration. Both bulk and ENM forms of ZnO significantly decreased basal soil respiration, 24.5 and 27.4%, respectively. No differences in basal respiration between bulk and ENM forms of metal oxides were observed.

Soil DNA

Soil DNA was decreased by nanoLi_2O (22%) and MoO_3 (13%, both bulk and ENM). In contrast, there was an increase of 12% in soil DNA under nanoZnO (Table 3). Neither NiO nor bulkZnO affected total soil DNA. When identifying total DNA response on specific days (Fig. S3C†), most of the DNA decreased in soil under nanoLi_2O exposure at the beginning of the experiment, with a gradual recovery to soil control levels by day 14. In contrast, DNA concentration in soils under MoO_3 (both bulk and ENM form) decreased with time, with no differences on specific days compared to the control. On the other hand, the overall significant increase in total DNA in soil under nanoZnO may be explained by the higher (but not significant) total DNA on days 7 and 14 of the experiment.

Soil microbial biomass

The quantity of phospholipid-phosphate (PL-PO_4) was used to evaluate the treatment effects on soil microbial biomass at days 1 and 14 after metal oxide application. PL-PO_4 was significantly 28% lower under the presence of bulkNiO compared to the control. In contrast, there was no difference on PL-PO_4 response in soils under the other metal oxides and the control; however, the overall response to bulk and ENM forms of all MoO_3, NiO, and ZnO varied (Table 3). There was a 43% difference in the PL-PO_4 response between bulk and ENM forms of MoO_3; while microbial biomass increased 21% compared to the control under bulkMoO_3, there was a 15% decrease compared to the control under nanoMoO_3. There was a 21% difference in the PL-PO_4 response between bulk and ENM forms of NiO; although both forms of NiO decreased microbial biomass, the effect of bulkNiO was stronger than that of nanoNiO. There was a 24% difference in the PL-PO_4 response between bulk and ENM forms of ZnO, while microbial biomass decreased 5% compared to the control under bulkZnO, there was a 24% increase compared to the control under nanoZnO. BulkMoO_3 yielded higher microbial biomass than nanoMoO_3 on day 1 but each treatment did not differ to the control (Fig. S3D†).

Soil microbial biomass was further analyzed using phospholipid fatty acids as total PLFAs, bacterial PLFAs, fungal PLFAs and fungal : bacteria (F : B) ratio on day 1 and 14 after metal oxide addition (Table 4, Fig. S4†). In general, microbial biomass increased in the presence of nanoLi_2O and bulkMoO_3, and decreased under NiO and ZnO. NanoLi_2O was the only metal oxide that significantly decreased microbial F : B, probably due to changes in a significant increase in bacterial PLFAs with no change in fungal PLFAs. Overall, there was no difference between bulk and ENM forms in soil microbial biomass response exposed to MoO_3 and NiO. However, total PLFAs, bacterial PLFAs, and fungal PLFAs response to bulkZnO was significantly lower than that for nanoZnO.

Trend in the total and bacterial PLFAs responses followed a similar pattern during day 1 and 14 (Fig. S4†). Response of

Table 4 Comparisons of soil microbial PLFAs under metal oxide exposure. Control was soil with no metal oxide addition. Post-hoc Dunnett's test was used to assess metal oxide (control *vs.* treatment) and size (bulk *vs.* ENM) effects

PLFAs group	Total PLFAs		Bacterial PLFAs		Fungal PLFAs		F : B	
	% change	*p*	% change	*p*	% change	*p*	% change	*p*
Control *vs.*								
NanoLi_2O	8.4	0.005	10.2	<0.001	3.4	0.767	−19.6	<0.001
BulkMoO_3	6.5	0.006	7.6	0.005	11.5	0.028	−2.1	0.852
NanoMoO_3	2.5	0.463	2.2	0.633	5.0	0.522	1.6	0.927
BulkNiO	−6.6	0.005	−7.2	0.005	−11.1	0.045	1.2	0.995
NanoNiO	−5.8	0.011	−5.8	0.022	−11.7	0.024	−3.5	0.783
BulkZnO	−9.2	<0.001	−9.3	<0.001	−18.8	<0.001	−5.6	0.424
NanoZnO	−3.2	0.267	−3.1	0.343	−6.0	0.408	−1.3	0.992
Bulk *vs.* ENM								
MoO_3	3.9	0.152	5.2	0.071	6.3	0.376	−3.7	0.638
NiO	−0.9	0.991	−1.5	0.951	0.7	0.999	4.5	0.766
ZnO	−6.2	0.012	−6.4	0.021	−13.7	0.018	−4.2	0.790

Table 5 Comparisons of soil microbial PLFAs groups under metal oxide exposure. Abundance PLFAs change (%) due to metal oxide (control *vs.* treatment) and size (bulk *vs.* ENM) and statistical significance (*p* value, post-hoc Dunnett's test) are presented

PLFAs group	Saturated straight-chain		Methyl branched		Monounsaturated		Cyclopropyl saturated		Terminally branched		Polyunsaturated	
	% change	*p*	% change	*p*	% change	*p*	% change	*p*	% change	*p*	% change	*p*
Control *vs.*												
NanoLi$_2$O	−1.9	0.636	30.1	0.104	0.0	1.000	−13.4	0.010	11.7	0.001	−37.6	0.042
BulkMoO$_3$	0.1	0.999	13.5	0.641	−3.5	0.300	−10.6	0.041	5.4	0.146	27.3	0.163
NanoMoO$_3$	−1.0	0.925	29.6	0.112	3.6	0.290	2.2	0.910	−5.5	0.145	−9.4	0.855
BulkNiO	1.3	0.909	−22.7	0.012	0.7	0.989	3.1	0.925	−2.5	0.819	0.0	1.000
NanoNiO	−1.3	0.897	−4.0	0.943	0.0	1.000	9.5	0.159	−2.1	0.866	−0.3	1.000
BulkZnO	−0.4	0.998	−27.2	0.001	−1.7	0.789	15.1	0.010	−2.8	0.735	10.4	0.503
NanoZnO	−3.1	0.331	−10.9	0.346	1.8	0.739	13.5	0.024	−5.1	0.241	3.4	0.979
Bulk *vs.* ENM												
MoO$_3$	1.1	0.937	−12.4	0.625	−6.9	0.012	−12.6	0.013	11.5	0.001	40.5	0.055
NiO	2.7	0.659	−19.5	0.079	0.7	0.996	−5.9	0.667	−0.3	1.000	0.3	1.000
ZnO	2.8	0.622	−18.2	0.133	−3.5	0.331	1.4	0.997	2.5	0.917	6.7	0.894

soil microbial biomass to nanoLi$_2$O was observable only on day 14; total PLFAs and bacterial PLFAs increased while F : B significantly decreased. Soils under bulkMoO$_3$ exposure significantly increased microbial biomass, including total PLFAs, bacterial PLFAs, and fungal PLFAs, on day 1, with no effect on day 14. Total PLFAs and fungal PLFAs significantly decreased under nanoNiO exposure on day 14 after metal oxide addition. Soils exposed to bulkZnO decreased total PLFAs, bacterial PLFAs and fungal PLFAs with no effect on F : B. There was no significant effect on soil microbial biomass after nanoMoO$_3$, bulkNiO, nor nanoZnO exposure.

Soil microbial phospholipid fatty acid (PLFA) composition

In general, metal oxides did not affect saturated straight chain PLFAs nor monounsaturated PLFAs (Table 5). NanoLi$_2$O significantly decreased the relative abundance of cyclopropyl saturated PLFAs (Gram-negative bacteria) and polyunsaturated PLFAs (fungi), while increasing terminally branched PLFAs (Gram-positive bacteria) abundance. Bulk forms of NiO and ZnO decreased the abundance of methyl branched PLFAs group (Gram-positive bacteria). BulkZnO and nanoZnO increased the abundance of cyclopropyl saturated PLFAs (Gram-negative bacteria), while bulkMoO$_3$ decreased it. Only MoO$_3$ produces a different soil response in terms of PLFA groups abundance between bulk and ENM form: bulkMoO$_3$ produced lower relative abundance in monounsaturated PLFAs (Gram-negative bacteria) and cyclopropyl saturated PLFAs (Gram-negative bacteria), while terminally branched PLFAs (Gram-positive bacteria) were significantly higher compared to nanoMoO$_3$.

The relative abundance of groups of PLFAs and individual PLFAs was also analyzed on days 1 and 14 after metal oxide application (Fig. S5†). Metal oxides did not affect the mean abundance of the PLFAs groups on the next day (day 1) after exposure. However, cyclopropyl saturated PLFAs, terminally branched PLFAs and polyunsaturated PLFAs in soil responded differently to bulk and ENM forms of MoO$_3$. These differences were mainly due to a more dramatic response to nanoMoO$_3$ in the individual PLFAs cy19:0, i15:0 and i17:0, and 18:2n6t (Fig. S6†). After 14 days of metal oxide exposure, nanoLi$_2$O, nanoNiO, and ZnO affected the mean abundance of soil PLFAs groups (Fig. S5†). An abundance of terminally branched PLFAs increased while polyunsaturated PLFAs decreased after nanoLi$_2$O, mainly reflected in the relative abundance of the individual PLFAs a15:0 and 18:2n6c (Fig. S6†). BulkZnO decreased the relative abundance of methyl branched PLFAs while increased cyclopropyl saturated PLFAs. NanoNiO and nanoZnO also increased the abundance of cyclopropyl saturated PLFAs. The differences in methyl branched PLFAs and cyclopropyl saturated PLFAs was mainly due to the relative abundance of individual PLFAs 10-Methyl18:0 and cy19:0, respectively.

Soil microbial community composition

16S rDNA gene V4/ITS1 survey resulted in a dataset of 30 908 430 reads. After demultiplexing and quality control, total sequences for 16S rDNA gene V4 and ITS1, were 2 948 723 and 6 137 054 reads, respectively. The median sequence length was 251 bp. For 16S rDNA gene V4, 3844 ASVs representing 33 phyla (Table S4†) were identified using 99% identity. Most (99.6%) of the sequences belonged to *Bacteria*, while the remaining (0.4%) belonged to *Archaea*. At a phylum level, the most abundant (>10%) belonged to *Bacteria* and were *Proteobacteria* (18.8%), *Bacteroidetes* (15.6%), and *Acidobacteria* (13.2%), while 19 phyla were identified at relatively low abundances (<1% of observed phyla). For ITS1, a total of 3332 ASVs representing 13 phyla (Table S4†) were identified using 97% identity. At a phylum level, the most abundant fungi were *Ascomycota* (48.9%), *Basidiomycota* (12.9%), *Mortierellomycota* (9.2%), and *Glomeromycota* (2.3%), while 24.2% were unidentified/unassigned, and eight phyla were identified at a relatively low abundance (<1%).

For the 16S rDNA gene V4, differential abundance analysis of phyla in soils revealed more pronounced responses to metal oxide exposure on day 14 (Fig. 1). Under nanoLi$_2$O exposure, the abundance of *Acidobacteria*

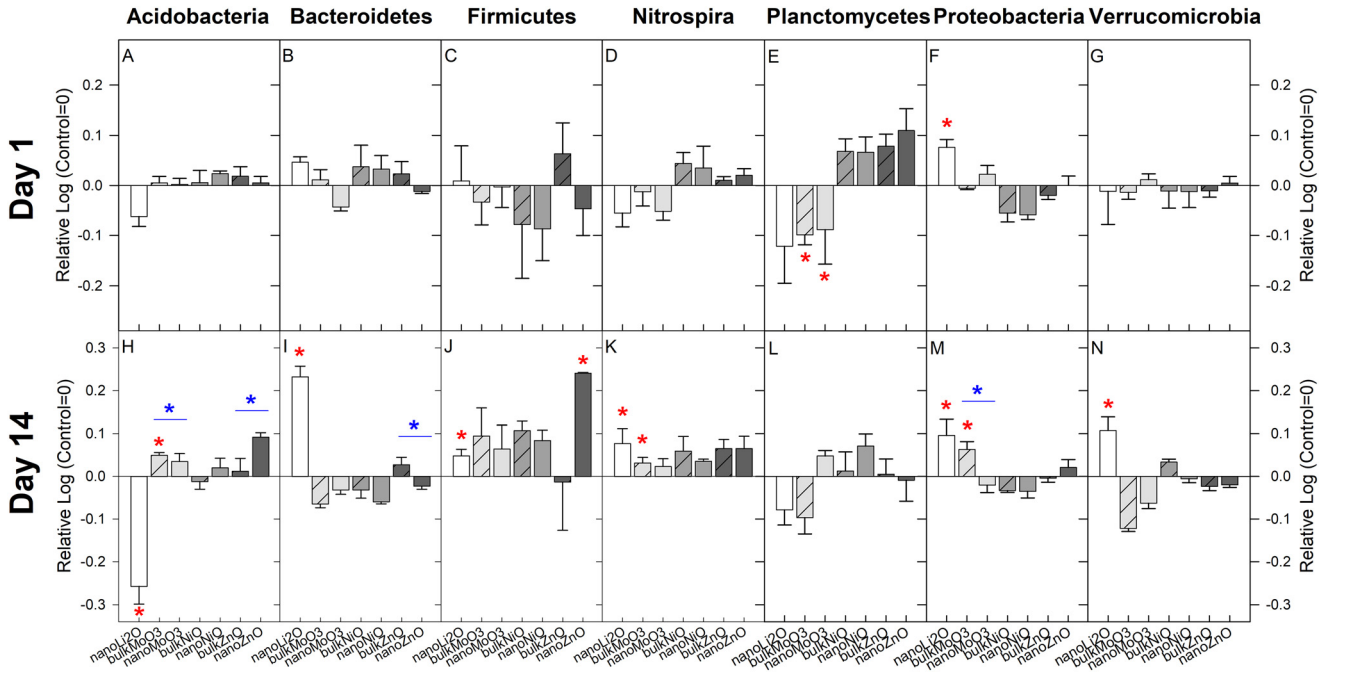

Fig. 1 Differential abundance analysis of prokaryotic (16S rDNA gene V4) phyla in soils at 1 (A–G) and 14 (H–N) days after metal oxide application. Control was soil with no metal oxide addition. Logarithm (base 10) of the relative response (*i.e.*, soil response to metal oxide/response of soil control) are presented, where positive and negative numbers represent an increase or decrease in activity, respectively. Error bars represent ±1 standard error (n = 3). Asterisk(s) and underlined asterisk(s) represent the significance of the treatment (metal oxide *vs.* control) and size (bulk *vs.* ENM) effect, respectively. One asterisk identifies significant differences ($p < 0.05$).

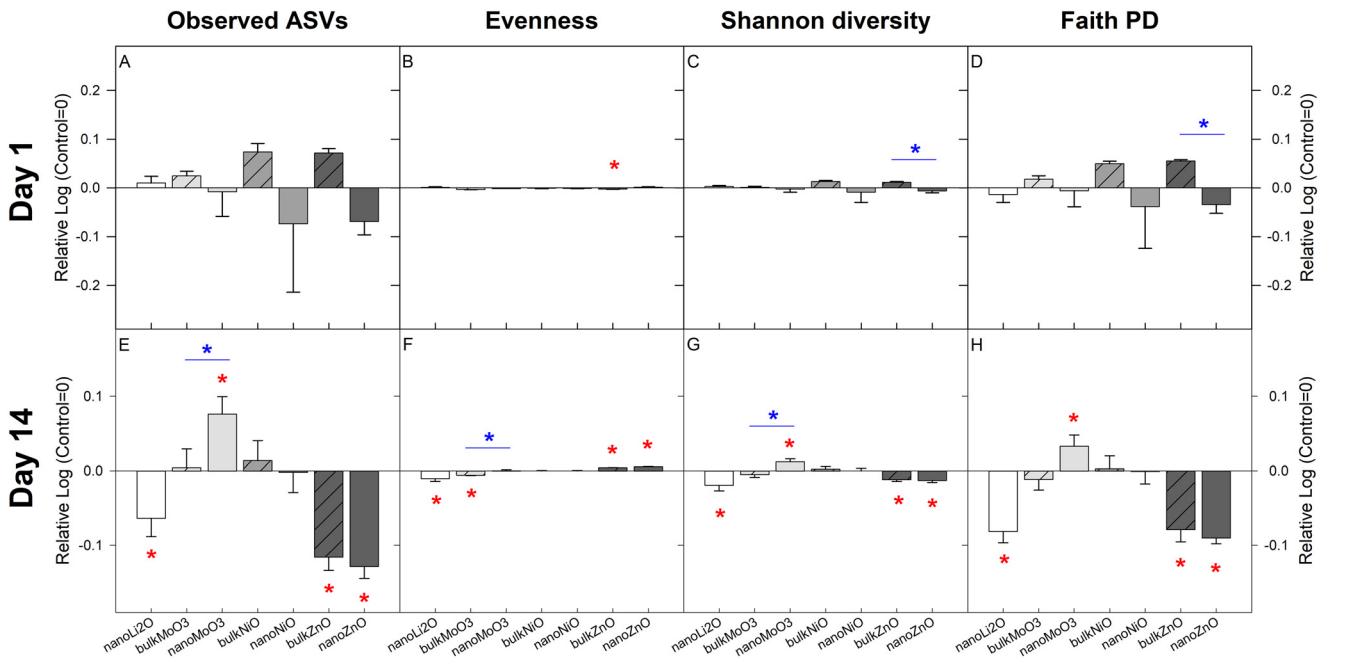

Fig. 2 Prokaryotic alpha diversity metrics of richness (observed ASVs, A and E), evenness (B and F), Shannon diversity (C and G), and Faith's Phylogenetic diversity (D and H), from soils 1 and 14 days after metal oxide exposure (n = 3). Control was soil with no metal oxide addition. Logarithm (base 10) of the relative response (*i.e.*, soil response to metal oxide/response of soil control) are presented, where positive and negative numbers represent an increase or decrease in activity, respectively. Error bars represent ±1 standard error (n = 3). Asterisk(s) and underlined asterisk(s) represent the significance of the treatment (metal oxide *vs.* control) and size (bulk *vs.* ENM) effect, respectively. One asterisk identifies significant differences ($p < 0.05$).

decreased while *Bacteroides*, *Firmicutes*, *Nitrospira*, *Proteobacteria*, and *Verrucomicrobia* increased. Compared to control soil, the relative abundance of *Acidobacteria*, *Nitrospira* and *Proteobacteria* was significantly increased in soils exposed to bulkMoO_3. The relative abundance of *Firmicutes* was also significantly higher after nanoZnO exposure with no differences with bulkZnO. The relative abundance of *Acidobacteria* was significantly higher after nanoZnO exposure while *Bacteroides* was significantly lower than that of nanoZnO. No significant differential abundances in phyla were observed after NiO exposure.

Differential abundance analysis of fungal (ITS1) phyla in soils exposed to metal oxides did not reveal significant patterns and no differences between bulk and ENM form were observed (Fig. S7†). After one day of exposure, MoO_3 and bulkZnO increased the abundance of *Mortierellomycota*, and bulkNiO increased the relative abundance of *Glomeromycota*, while nanoZnO decreased the abundance of *Kickxellomycota*. After 14 days of exposure, the relative abundance of *Mortierellomycota* and *Kickxellomycota* were decreased by nanoZnO and nanoNiO, respectively.

Soil microbial diversity

Alpha diversity in bacterial communities was clearly more affected after 14 days of metal oxide exposure (Fig. 2). After 14 days, richness decreased under nanoLi_2O and ZnO (bulk and ENM form), and increased after nanoMoO_3 exposure. Community evenness decreased under nanoLi_2O and bulkMoO_3, while increasing when soil was exposed to ZnO (both bulk and ENM). Exposure to nanoLi_2O and ZnO resulted in a decrease of Shannon and Faith's PD metrics, while exposure to nanoMoO_3 resulted in an increase of those metrics. Similarly, fungal alpha diversity was more affected after 14 days of metal oxide exposure (Fig. 3). Exposure to nanoLi_2O and bulkZnO resulted in a decrease in richness and evenness, respectively, while exposure to bulkMoO_3 decreased richness, evenness, and Shannon diversity.

When analyzing variability between samples (beta diversity, Table 6 and Fig. S8†), no significant differences between soil microbial communities exposed to metal oxides (control *vs.* metal oxide) or between size (bulk *vs.* ENM) were observed.

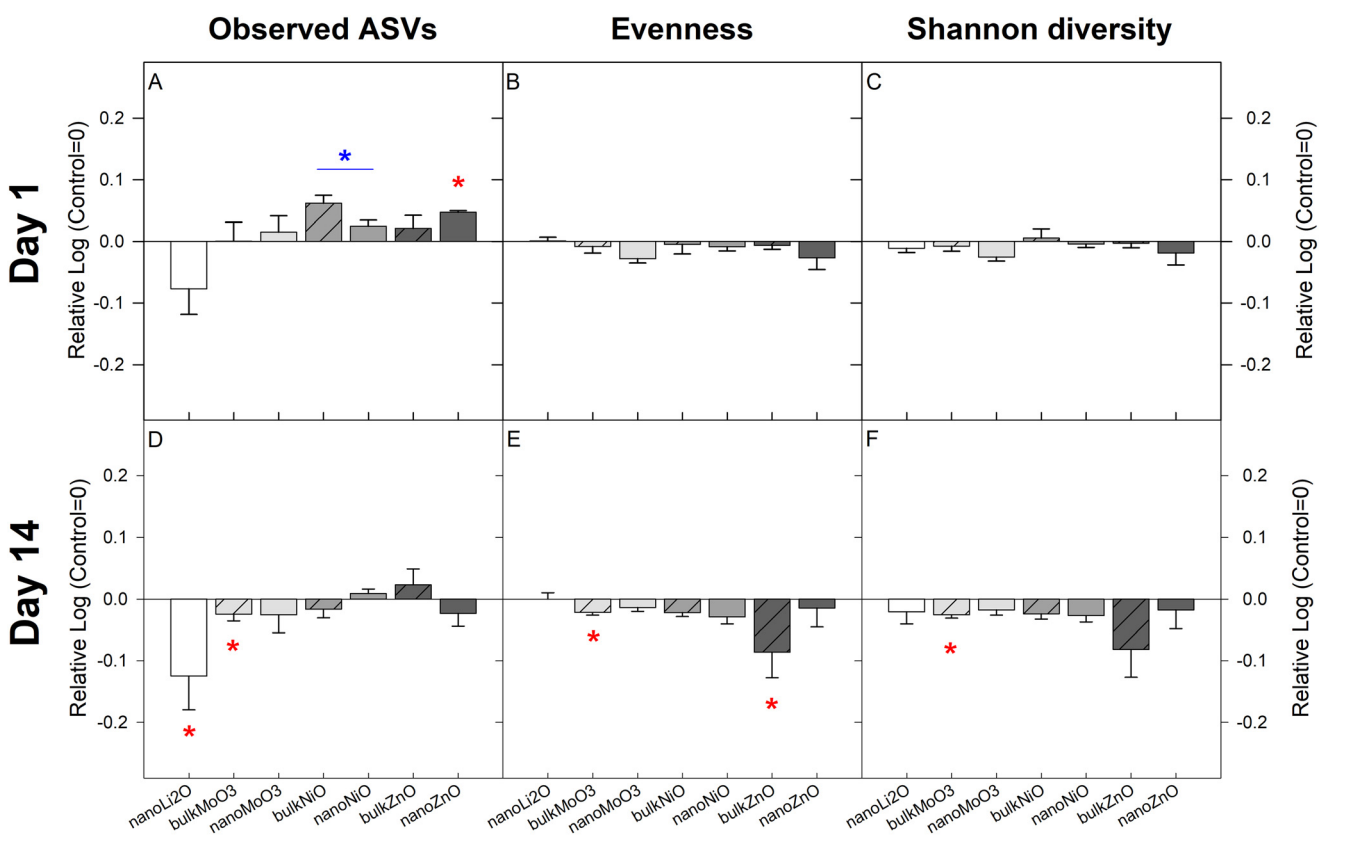

Fig. 3 Fungal community alpha diversity metrics of richness (observed ASVs, A and D), evenness (B and E), and Shannon diversity (C and F); from soils 1 and 14 days after metal oxide exposure (n = 3). Control was soil with no metal oxide addition. Logarithm (base 10) of the relative response (*i.e.*, soil response to metal oxide/response of soil control) are presented, where positive and negative numbers represent an increase or decrease in activity, respectively. Error bars represent ±1 standard error (n = 3). Asterisk(s) and underlined asterisk(s) represent the significance of the treatment (metal oxide *vs.* control) and size (bulk *vs.* ENM) effect, respectively. One asterisk identifies significant differences ($p < 0.05$).

Table 6 Significance (*p*-value, PERMANOVA-Kruskal–Wallis) of β-diversity (*i.e.*, between sample diversity) metrics *via* 16S rDNA gene V4 and ITS1 amplicons on soil microbial communities 1 and 14 days after metal oxides exposure. Treatment (*i.e.*, control *vs.* metal oxide) and size (bulk *vs.* ENM) effects are presented

	16S rDNA gene V4							ITS1			
	Day 1				Day 14			Day 1		Day 14	
	Jaccard	Bray-Curtis	Unweighted-Unifrac	Weighted-Unifrac	Jaccard	Bray-Curtis	Unweighted-Unifrac	Weighted-Unifrac	Jaccard	Bray-Curtis	Jaccard	Bray-Curtis
Control *vs.*												
$NanoLi_2O$	0.095	0.097	0.106	0.109	0.102	0.092	0.085	0.092	0.208	0.711	0.114	0.098
$BulkMoO_3$	0.100	0.105	0.209	0.199	0.091	0.088	0.806	0.095	0.099	0.568	0.202	0.586
$NanoMoO_3$	0.395	0.105	0.187	0.102	0.103	0.096	0.112	0.103	0.321	0.792	0.808	0.801
BulkNiO	0.624	1.000	0.716	0.693	0.515	0.201	0.196	0.105	0.105	0.112	0.195	0.295
NanoNiO	0.790	0.614	1.000	0.320	0.426	0.408	0.612	0.106	0.704	0.487	0.396	0.416
BulkZnO	0.886	0.493	0.801	0.907	0.113	0.094	0.099	0.103	0.112	0.105	0.194	0.101
NanoZnO	0.430	0.405	1.000	0.318	0.108	0.091	0.103	0.104	0.598	0.619	0.104	0.191
Bulk *vs.* ENM												
MoO_3	0.688	0.284	0.389	0.110	0.102	0.095	0.406	0.116	1.000	0.600	0.198	0.324
NiO	0.589	0.595	0.910	0.789	0.384	0.706	0.200	0.287	0.097	0.209	0.717	0.782
ZnO	0.099	0.102	0.102	0.706	0.783	0.108	0.691	0.097	0.182	0.402	0.904	0.097

Discussion

Solubility and pH in aqueous media depend on metal oxide type and size

One factor for metal oxide ENMs toxicity might be the release of metal ions and their inherent toxicity.[45,46] Understanding the dissolution behavior is important, particularly when the metal oxide might encounter water or other aqueous solutions (*e.g.*, soil pore water). The dissolution of ENMs is an important property that influences their environmental persistence and impact.[47] The amount of metal ion release, together with other properties such as surface charge, aggregation state, and size distribution, differ considerably depending on the composition of the aqueous medium/matrix into which the metal oxide ENMs are placed.[48] Due to challenges tracking these characteristics in complex matrices (such as soil), we evaluated the solubility of metal oxides and their influence on pH in saline solution (SS) and a nutritionally rich medium (Luria-Bertani, LB) to understand their behavior in aqueous solution, as in soil they will likely encounter soil pore water. However, metal oxide ENM chemical reactions may be more complex in the soil matrix,[48–50] where dissolution in the soil can be promoted by the interaction of metal ions with soil components, such as organic matter, potentially reducing their bioavailability and toxicity.[51,52]

In this study, solubility and final pH varied depending on the metal oxide investigated. $BulkMoO_3$ was highly soluble in SS with a significant pH decrease and somewhat soluble in LB with no effect on pH. $BulkMoO_3$ is expected to have limited solubility in the water below neutral pH,[53] but the presence of NaCl (specifically Cl^-) in SS may have enhanced its solubility due to the formation of Cl^- complexes, such as the case for another metal cation, Cd(II).[54] The presence of organic matter in LB medium may have limited $bulkMoO_3$ dissolution by obscuring the particle surface and restricting the diffusion of released ions.[51] $NanoMoO_3$ was poorly soluble in either of the aqueous solutions but showed a significant decrease in SS pH while an increase in LB pH. Although not evaluated in the same solutions, another study found that $nanoMoO_3$ (100 μg mL^{-1} as metal content) resulted in immediate partial dissolution in DI water (34.9%), root exudates (31.3%), and soil leachate (33.7%).[48] $NanoMoO_3$ was also found to be highly soluble (48.5%) in a culture medium.[45] NanoNiO and nanoZnO are described as water insoluble in material safety data sheets. NanoNiO used in this study was only slightly soluble (0.52 mg Ni mL^{-1}, <2%) in both solutions, while both forms of ZnO were highly soluble in LB medium and somehow soluble in SS. Although there were differences in solubility between ENM and bulk form for NiO and ZnO, a significant increase in the pH for both solutions was observed, with a stronger response in SS than LB, reflecting LB buffer capacity. The difference in solubility and pH response might be due to the initial pH of each solution and the presence of organic matter/salts.[46] Both nanoNiO and nanoZnO were previously reported as

slightly soluble (1.04% and 1.63%, respectively) in a culture medium,[45] however, we report high solubility (>38 μg Zn mL^{-1}, >95%) of ZnO in LB. Toxicity effects of nanoNiO had been attributed to the nanoparticles themselves than due to the release of Ni ions.[46] In contrast, toxicity of nanoZnO has been attributed mainly due to the released Zn^{2+},[20,46] although no differences in dissolution between ENM and bulk forms were observed here. Overall, our contrasting results compared to other reports highlight the importance of evaluating the dissolution of the specific compounds in the study as they can differ between manufacturers or product lot.[55]

LB medium had been used to isolate microorganisms from soil to investigate their biotechnological potential[56–58] or to understand the toxicity of chemical agents, such as ENMs.[59–62] Future studies, however, need to consider aqueous solutions more environmentally relevant with closer characteristics to the matrix in the study. In the case of soils, the use of soil extract might provide a closer simulation to understand the behavior of metal oxides for solubility and effects on pH in the soil pore water. Beyond solubility and acid–base character (pH) effect, other characteristics of ENMs (*e.g.*, size, shape, charge), as well as soil properties (*e.g.*, cation exchange capacity, soil particle size distribution, organic matter, clay content), will determine physical and chemical processes possibly resulting in ENM dissolution, agglomeration, and/or aggregation.[63] These reactions might reduce their bioavailability and toxicity to the soil biota. Such ENM reactions in the soil matrix remain to be explored.

Size of metal oxide did not drive soil response

ENMs are expected to be more toxic than their bulk counterpart due to their small size, high specific surface area, greater surface reactivity, and potential ability to penetrate cell walls.[64] These properties of ENMs could facilitate penetration to microbes in soil micropores, producing detrimental effects on microbial functionality.[49,65] However, ENMs may undergo chemical transformation once in soil, causing aggregation and/or interaction with soil components (*e.g.*, organic matter), thus reducing their toxic effects.[49,50] Further, the toxicity of ENMs also depends on the ability of microbial adsorption and the specific sensitivity of microbial species.[45,66] In this study, we provided evidence that soil is influenced by the presence of nanoLi_2O, nanoMoO_3, and nanoZnO. However, through the assessment of the toxicity provided here, there is not enough evidence that soil toxicity was caused exclusively by nano-effects.

The most notable soil response was to nanoLi_2O, which caused a drastic increase in pH (2.83 units), as well as an increase in basal respiration and microbial biomass, while decreased soil enzyme activity involved in carbon, nitrogen, and phosphorus cycling, total soil DNA, fungal : bacterial biomass ratio, and prokaryotic alpha diversity and fungal richness. Furthermore, under nanoLi_2O exposure, the relative abundance of *Acidobacteria* decreased while *Bacteroidetes*, *Firmicutes*, *Nitrospirae*, *Proteobacteria,* and *Verrucomicrobia* increased. These findings aligned with several reports where changes in soil pH were correlated with changes in relative microbial abundance, with *Acidobacteria* decreasing as pH increased[67] while *Firmicutes*,[68] *Nitrospirae*,[69] *Verrucomicrobia*,[69] *Bacteroidetes*,[70–72] and *Proteobacteria*[70–72] were positively correlated with soil pH. The relative abundance of fungal phyla was not affected by nanoLi_2O. Fungi are less responsive to pH than bacteria.[67,68,71] In general, fungi have a more comprehensive optimum pH (5–9 units) without significantly inhibiting their growth.[67] In fact, changes in the fungal community due to changes in soil pH might indirectly respond to the competitive influence of the highly dynamic bacterial community along the pH gradient.[67,73] Since lithium ions are expected to be more bioavailable in acidic soils compared to alkaline conditions,[74] our results support the hypothesis of indirect soil effects by Li_2O (both bulk and ENM form) due to a drastic pH shift.[15] When mixed with water, Li_2O forms LiOH in an exogenic reaction where one unit of Li_2O gives two units of LiOH.[75] LiOH is considered a strong base even with a pK_b of −0.04. The mechanism of LiOH formation was recently considered by Weber *et al.*[76] They demonstrated that a Li_2O crystal in water becomes surrounded by layers of LiOH, and the kinetics of dissolution is controlled by the movement of water through the LiOH layers. LiOH shell expands as water is added to the crystal surface; LiOH on the outside of the structure is lost to bulk water, increasing pH.

Characteristics of the soil bacteria with changes in relative abundance due to nanoLi_2O appeared to reflect the response not only to pH but also possibly to organic matter/nutrient availability. Besides changes in microbial metabolism, altered pH may produce changes in other soil characteristics, such as organic carbon and nitrogen content, nutrient availability, and physical properties.[68,71,77] In fact, pH represents a direct physiological constraint on soil-inhabiting bacteria, altering the dynamic between individual taxa whose growth, competitiveness, and survival might be affected if the soil pH extends beyond a given range.[71] In this context, *Acidobacteria* are oligotrophs characterized by slow growth rates and the metabolism of more refractory carbon substrates.[73] Although members of *Acidobacteria* are present in environments with various pH conditions, phylogenetic diversity within the phylum generally decreases as soil pH differs from neutrality.[71,72,78] *Firmicutes* are copiotrophic bacteria generally abundant in soils.[79] In soils with a drastic pH increase, *Firmicutes* became the dominant group rapidly (16 h), along with higher soil denitrification potential, dissimilatory nitrate reduction to ammonium, and organic matter mineralization.[68] The phylum *Nitrospirae* comprises aerobic chemolithotrophs participating in the nitrogen cycle (nitrification). As soil pH increased due to biochar amendments, pH and total nitrogen content were the most influential factors on the dominant *Nitrospirae*,[69] increasing nitrification activity, and total N content. The phylum *Verrucomicrobia* is ubiquitous in soils and significantly

correlated with soil pH (r = 0.72, $p < 0.001$) and carbon/nitrogen ratio (C : N ratio).[80] *Bacteroidetes* comprises a large group of Gram-negative bacteria with a wide range of physiological types (*e.g.*, from strict anaerobes such as *Bacteroides*, to strict aerobes such as *Flavobacteria*), considered as specialists for high-molecular-weight organic matter (proteins and carbohydrates) degradation.[81,82] Lastly, *Proteobacteria* are key players in nutrient cycling, especially in nutrient-rich ecosystems.[73] Soil properties (*e.g.*, organic carbon and nitrogen content, nutrient availability, and physical properties) and microbial metabolism (*e.g.*, organic matter mineralization, denitrification potential) response to nanoLi_2O exposure remain to be understood.

In terms of MoO_3, both bulk and ENM form of MoO_3 decreased total DNA and acid phosphatase activity. Bacterial (evenness) and fungal (richness, evenness and Shannon diversity) soil diversity decreased in the presence of bulkMoO_3. Under bulkMoO_3 exposure, *Acidobacteria*, *Nitrospira*, and *Proteobacteria* abundance increased, probably as a response to the slight decrease in soil pH,[78] or to molybdenum ions as those are expected to present a low absorption by the soil.[83] In the presence of nanoMoO_3, bacterial community richness, Shannon diversity, and Faith's PD metrics increased. If not soluble in the soil matrix (as in SS or LB medium), bacterial alpha diversity response might be due to a nanosized effect from nanoMoO_3.

NiO did not affect soil function in terms of enzyme activity or basal soil respiration but decreased bacterial and fungal biomass. However, NiO did not influence microbial (bacterial and fungal) community structure, diversity, or composition. While bulk and ENM form of NiO decreased overall soil pH, this was only by 0.11 and 0.14 units, respectively. BulkNiO dissolution was negligible in SS or LB medium but nanoNiO was slightly soluble in those media. If there is any dissolution in the soil matrix, nickel ions toxicity might be rendered by soil absorption due to high affinity for organic matter.[84]

As ZnO, both ENM and bulk form increased soil pH (0.2 units), microbial biomass of Gram-negative (*e.g.*, cy19:0) bacteria, and bacterial evenness, while decreased soil basal respiration and bacterial richness, Shannon diversity, and Faith's PD. The impact of ZnO on soil pH was likely due to their high dissolution rate (releasing OH^-).[85] Soils under bulkZnO decreased bacterial biomass, fungal biomass, and evenness. On the other hand, nanoZnO disturbed soil BG and NAG enzyme activity, increasing total DNA and soil bacterial members of the phylum *Firmicutes*. The presence of heavy metals (*i.e.*, Zn^{2+}) could inhibit soil enzyme activity by binding with either the active groups of the enzymes or the substrates.[86] Differences in the relative abundance of *Acidobacteria* and *Bacteriodetes* between ENM and bulk forms of ZnO were also observed, but those responses were not different from the control soil.

In general, we did not observe statistical differences between metal oxide treatments and control soil in prokaryotic or fungal communities, probably due to low sample replicates, n = 3. In our earlier study, we reported that nanoLi_2O, nanoMoO_3, and nanoNiO disturb the microbial community structure of the three domains of life.[15] However, we previously used the denaturing gradient gel electrophoresis (DGGE) technique, which provided information on ribotypes responses with a resolution that might not describe the complete microbial diversity.[87] DGGE inherent bias on the number and intensity of the DNA bands include i. co-migration of phylogenetically heterogeneous bands; ii. one organism may produce more than one band due to multiple, heterogeneous rDNA operons; and iii. the less abundant sequences might not amplify sufficiently to be visualized as bands on a DGGE gel.[88,89] Since we observed response to metal oxide on soil function and the relative abundance of taxa, future studies need to include higher number of biological replicates to quantitatively detect differences in the diversity of highly complex soil microbial communities analyzed using high-throughput DNA sequencing reads.

Conclusion

The soil response depended on the metal oxide in consideration. The type and potential concentration of the released metal as well as the influence on soil pH appeared to be a more substantial factor than the size (bulk or ENM) of the compound. Furthermore, the effect of nanoLi_2O appeared to be driven by a rapid and drastic increase in soil pH. However, ENMs behavior in the soil matrix that may reduce bioavailability and toxicity to the soil biota remain to be explored. Although neither of our studies addressed how long the Li_2O remains active in the system, this work and our past efforts support a conclusion of caution around the possible introduction of Li_2O to the environment. We also suggest that similar considerations be taken when applying soil amendments that cause substantial soil pH changes (*e.g.*, biochar, lime, wood ashes).

Conflicts of interest

There are no conflicts to declare.

Acknowledgements

This work was supported by the Purdue-Colciencias agreement under Colombia-Purdue Institute for Advanced Scientific Research – (CPIASR) and the Winifred B. Bilsland Interdisciplinary Doctoral Dissertation Fellowship for Agronomy and the Ecological Sciences and Engineering Program at Purdue. The authors are also grateful for the support from the Department of Statistics at Purdue University, especially Dr. Evidence Matangi, for the assistance with data analysis.

References

1 M. Baalousha, Y. Yang, M. E. Vance, B. P. Colman, S. McNeal, J. Xu, J. Blaszczak, M. Steele, E. Bernhardt and M. F. Hochella Jr, *Sci. Total Environ.*, 2016, **557–558**, 740–753.

2 F. Gottschalk and B. Nowack, *J. Environ. Monit.*, 2011, **13**, 1145–1155.
3 A. A. Keller, S. McFerran, A. Lazareva and S. Suh, *J. Nanopart. Res.*, 2013, **15**, 1–17.
4 M. Kah, *Front. Chem.*, 2015, **3**, 64.
5 D. F. Bezdicek, R. I. Papendick and R. Lal, in *Methods for Assessing Soil Quality*, ed. J. W. Doran and A. J. Jones, Soil Science Society of America, Inc., Madison, Wisconsin, USA, 1996, DOI: **10.2136/sssaspecpub49.introduction**.
6 P. R. Hirsch, T. H. Mauchline and I. M. Clark, in *Molecular Microbial Ecology of the Rhizosphere*, ed. F. J. de Bruijn, John Wiley & Sons, Inc., Hoboken, NJ, USA, 2013, vol. 1 & 2, pp. 45–55.
7 H. Nacke, C. Fischer, A. Thürmer, P. Meinicke and R. Daniel, *Microb. Ecol.*, 2014, **67**, 919–930.
8 J. W. Doran and M. R. Zeiss, *Appl. Soil Ecol.*, 2000, **15**, 3–11.
9 S. Frenk, T. Ben-Moshe, I. Dror, B. Berkowitz and D. Minz, *PLoS One*, 2013, **8**, e84441.
10 P. A. Holden, J. P. Schimel and H. A. Godwin, *Curr. Opin. Biotechnol.*, 2014, **27**, 73–78.
11 C. Fajardo, M. L. Saccà, G. Costa, M. Nande and M. Martin, *Sci. Total Environ.*, 2014, **473–474**, 254–261.
12 N. Y. Taran, O. M. Gonchar, K. G. Lopatko, L. M. Batsmanova, M. V. Patyka and M. V. Volkogon, *Nanoscale Res. Lett.*, 2014, **9**, 289.
13 H. Chhipa, *Environ. Chem. Lett.*, 2017, **15**, 15–22.
14 H. Chhipa and P. Joshi, in *Nanoscience in Food and Agriculture 1*, ed. S. Ranjan, N. Dasgupta and E. Lichtfouse, Springer International Publishing, Cham, 2016, ch. 9, pp. 247–282, DOI: **10.1007/978-3-319-39303-2_9**.
15 H. Avila-Arias, L. F. Nies, M. B. Gray and R. F. Turco, *Sci. Total Environ.*, 2019, **652**, 202–211.
16 K. Chander and P. C. Brookes, *Soil Biol. Biochem.*, 1991, **23**, 927–932.
17 Y. Ge, J. H. Priester, L. C. Van De Werfhorst, S. L. Walker, R. M. Nisbet, Y.-J. An, J. P. Schimel, J. L. Gardea-Torresdey and P. A. Holden, *Environ. Sci. Technol.*, 2014, **48**, 13489–13496.
18 Y. Ge, J. P. Schimel and P. A. Holden, *Environ. Sci. Technol.*, 2011, **45**, 1659–1664.
19 Y. Ge, J. P. Schimel and P. A. Holden, *Appl. Environ. Microbiol.*, 2012, **78**, 6749–6758.
20 M. Li, L. Zhu and D. Lin, *Environ. Sci. Technol.*, 2011, **45**, 1977–1983.
21 K. R. Saiya-Cork, R. L. Sinsabaugh and D. R. Zak, *Soil Biol. Biochem.*, 2002, **34**, 1309–1315.
22 G. A. Smith, J. S. Nickels, B. D. Kerger, J. D. Davis, S. P. Collins, J. T. Wilson, J. F. McNabb and D. C. White, *Can. J. Microbiol.*, 1986, **32**, 104–111.
23 R. H. Findlay, G. M. King and L. Watling, *Appl. Environ. Microbiol.*, 1989, **55**, 2888–2893.
24 V. Acosta-Martínez, Z. Reicher, M. Bischoff and R. F. Turco, *Biol. Fertil. Soils*, 1999, **29**, 55–61.
25 J. B. Guckert, C. P. Antworth, P. D. Nichols and D. C. White, *FEMS Microbiol. Ecol.*, 1985, **1**, 147–158.
26 A. D. Peacock and D. C. White, in *Hydrocarbon and Lipid Microbiology Protocols: Microbial Quantitation, Community Profiling and Array Approaches*, ed. T. J. McGenity, K. N. Timmis and B. Nogales, Springer Berlin Heidelberg, Berlin, Heidelberg, 2017, pp. 65–76, DOI: **10.1007/8623_2016_213**.
27 L. Liu, P. Gundersen, W. Zhang, T. Zhang, H. Chen and J. Mo, *Sci. Rep.*, 2015, **5**, 14378.
28 A. Frostegård and E. Bååth, *Biol. Fertil. Soils*, 1996, **22**, 59–65.
29 N. Lewe, S. Hermans, G. Lear, L. T. Kelly, G. Thomson-Laing, B. Weisbrod, S. A. Wood, R. A. Keyzers and J. R. Deslippe, *J. Microbiol. Methods*, 2021, **188**, 106271.
30 Å. Frostegård, A. Tunlid and E. Bååth, *Soil Biol. Biochem.*, 2011, **43**, 1621–1625.
31 J. G. Caporaso, C. L. Lauber, W. A. Walters, D. Berg-Lyons, J. Huntley, N. Fierer, S. M. Owens, J. Betley, L. Fraser, M. Bauer, N. Gormley, J. A. Gilbert, G. Smith and R. Knight, *ISME J.*, 2012, **6**, 1621–1624.
32 J. G. Caporaso, C. L. Lauber, W. A. Walters, D. Berg-Lyons, C. A. Lozupone, P. J. Turnbaugh, N. Fierer and R. Knight, *Proc. Natl. Acad. Sci.*, 2011, **108**, 4516–4522.
33 A. M. Bolger, M. Lohse and B. Usadel, *Bioinformatics*, 2014, **30**, 2114–2120.
34 J. G. Caporaso, J. Kuczynski, J. Stombaugh, K. Bittinger, F. D. Bushman, E. K. Costello, N. Fierer, A. G. Pena, J. K. Goodrich, J. I. Gordon, G. A. Huttley, S. T. Kelley, D. Knights, J. E. Koenig, R. E. Ley, C. A. Lozupone, D. McDonald, B. D. Muegge, M. Pirrung, J. Reeder, J. R. Sevinsky, P. J. Turnbaugh, W. A. Walters, J. Widmann, T. Yatsunenko, J. Zaneveld and R. Knight, *Nat. Methods*, 2010, **7**, 335–336.
35 B. J. Callahan, P. J. McMurdie, M. J. Rosen, A. W. Han, A. J. A. Johnson and S. P. Holmes, *Nat. Methods*, 2016, **13**, 581–583.
36 F. Pedregosa, G. Varoquaux, A. Gramfort, V. Michel, B. Thirion, O. Grisel, M. Blondel, P. Prettenhofer, R. Weiss, V. Dubourg, J. Vanderplas, A. Passos, D. Cournapeau, M. Brucher, M. Perrot and É. Duchesnay, *J. Mach. Learn. Res.*, 2011, **12**, 2825–2830.
37 C. Quast, E. Pruesse, P. Yilmaz, J. Gerken, T. Schweer, P. Yarza, J. Peplies and F. O. Glöckner, *Nucleic Acids Res.*, 2012, **41**, D590–D596.
38 P. Yilmaz, L. W. Parfrey, P. Yarza, J. Gerken, E. Pruesse, C. Quast, T. Schweer, J. Peplies, W. Ludwig and F. O. Glöckner, *Nucleic Acids Res.*, 2013, **42**, D643–D648.
39 F. O. Glöckner, P. Yilmaz, C. Quast, J. Gerken, A. Beccati, A. Ciuprina, G. Bruns, P. Yarza, J. Peplies, R. Westram and W. Ludwig, *J. Biotechnol.*, 2017, **261**, 169–176.
40 R. H. Nilsson, K.-H. Larsson, A. F. S. Taylor, J. Bengtsson-Palme, T. S. Jeppesen, D. Schigel, P. Kennedy, K. Picard, F. O. Glöckner, L. Tedersoo, I. Saar, U. Kõljalg and K. Abarenkov, *Nucleic Acids Res.*, 2018, **47**, D259–D264.
41 Y. Vázquez-Baeza, M. Pirrung, A. Gonzalez and R. Knight, *GigaScience*, 2013, **2**, 16.
42 M. I. Love, W. Huber and S. Anders, *Genome Biol.*, 2014, **15**, 550.
43 J. Chong, P. Liu, G. Zhou and J. Xia, *Nat. Protoc.*, 2020, **15**, 799–821.

44 A. Dhariwal, J. Chong, S. Habib, I. L. King, L. B. Agellon and J. Xia, *Nucleic Acids Res.*, 2017, **45**, W180–W188.
45 M. Horie, K. Fujita, H. Kato, S. Endoh, K. Nishio, L. K. Komaba, A. Nakamura, A. Miyauchi, S. Kinugasa, Y. Hagihara, E. Niki, Y. Yoshida and H. Iwahashi, *Metallomics*, 2012, **4**, 350–360.
46 D. Wang, Z. Lin, T. Wang, Z. Yao, M. Qin, S. Zheng and W. Lu, *J. Hazard. Mater.*, 2016, **308**, 328–334.
47 S. K. Misra, A. Dybowska, D. Berhanu, S. N. Luoma and E. Valsami-Jones, *Sci. Total Environ.*, 2012, **438**, 225–232.
48 P. Cervantes-Avilés, X. Huang and A. A. Keller, *Environ. Sci. Technol.*, 2021, **55**, 13443–13451.
49 M. Simonin and A. Richaume, *Environ. Sci. Pollut. Res.*, 2015, **22**, 13710–13723.
50 G. E. Schaumann, T. Baumann, F. Lang, G. Metreveli and H.-J. Vogel, *Sci. Total Environ.*, 2015, **535**, 1–2.
51 H. McShane, *Doctor of Philosophy thesis*, McGill University, 2013.
52 A. A. Keller, H. Wang, D. Zhou, H. S. Lenihan, G. Cherr, B. J. Cardinale, R. Miller and Z. Ji, *Environ. Sci. Technol.*, 2010, **44**, 1962–1967.
53 T. N. Angelidis, E. Tourasanidis, E. Marinou and G. A. Stalidis, *Resour., Conserv. Recycl.*, 1995, **13**, 269–282.
54 U. J. López-Chuken, U. López-Domínguez, R. Parra-Saldivar, E. Moreno-Jiménez, L. Hinojosa-Reyes, J. L. Guzmán-Mar and E. Olivares-Sáenz, *Int. J. Environ. Sci. Technol.*, 2012, **9**, 69–77.
55 M. Yamada, S. Takahashi, H. Sato, T. Kondo, T. Kikuchi, K. Furuya and I. Tanaka, *Biol. Trace Elem. Res.*, 1993, **36**, 89–98.
56 E. Dell'Amico, L. Cavalca and V. Andreoni, *FEMS Microbiol. Ecol.*, 2005, **52**, 153–162.
57 A. Ueno, Y. Ito, I. Yumoto and H. Okuyama, *World J. Microbiol. Biotechnol.*, 2007, **23**, 1739–1745.
58 M. Dimova, G. Iutynska, N. Yamborko, D. Dordevic and I. Kushkevych, *Processes*, 2022, **10**, 2170.
59 T. A. Qiu, T. H. T. Nguyen, N. V. Hudson-Smith, P. L. Clement, D.-C. Forester, H. Frew, M. N. Hang, C. J. Murphy, R. J. Hamers, Z. V. Feng and C. L. Haynes, *Anal. Chem.*, 2017, **89**, 2057–2064.
60 I. De Leersnyder, L. De Gelder, I. Van Driessche and P. Vermeir, *Nanomaterials*, 2019, **9**, 1684.
61 A. D. Samarajeewa, J. R. Velicogna, J. I. Princz, R. M. Subasinghe, R. P. Scroggins and L. A. Beaudette, *Environ. Pollut.*, 2017, **220**, 504–513.
62 Z. Ji, X. Jin, S. George, T. Xia, H. Meng, X. Wang, E. Suarez, H. Zhang, E. M. V. Hoek, H. Godwin, A. E. Nel and J. I. Zink, *Environ. Sci. Technol.*, 2010, **44**, 7309–7314.
63 P. S. Tourinho, C. A. M. van Gestel, S. Lofts, C. Svendsen, A. M. V. M. Soares and S. Loureiro, *Environ. Toxicol. Chem.*, 2012, **31**, 1679–1692.
64 P. A. Holden, J. L. Gardea-Torresdey, F. Klaessig, R. F. Turco, M. Mortimer, K. Hund-Rinke, E. A. Cohen Hubal, D. Avery, D. Barceló, R. Behra, Y. Cohen, L. Deydier-Stephan, P. L. Ferguson, T. F. Fernandes, B. Herr Harthorn, W. M. Henderson, R. A. Hoke, D. Hristozov, J. M. Johnston, A. B. Kane, L. Kapustka, A. A. Keller, H. S. Lenihan, W. Lovell, C. J. Murphy, R. M. Nisbet, E. J. Petersen, E. R. Salinas, M. Scheringer, M. Sharma, D. E. Speed, Y. Sultan, P. Westerhoff, J. C. White, M. R. Wiesner, E. M. Wong, B. Xing, M. Steele Horan, H. A. Godwin and A. E. Nel, *Environ. Sci. Technol.*, 2016, **50**, 6124–6145.
65 L. Vittori Antisari, S. Carbone, A. Gatti, G. Vianello and P. Nannipieri, *Soil Biol. Biochem.*, 2013, **60**, 87–94.
66 Y.-W. Baek and Y.-J. An, *Sci. Total Environ.*, 2011, **409**, 1603–1608.
67 J. Rousk, E. Baath, P. C. Brookes, C. L. Lauber, C. Lozupone, J. G. Caporaso, R. Knight and N. Fierer, *ISME J.*, 2010, **4**, 1340–1351.
68 C. R. Anderson, M. E. Peterson, R. A. Frampton, S. R. Bulman, S. Keenan and D. Curtin, *PeerJ Prepr.*, 2018, **6**, e6090.
69 S. Fan, J. Zuo and H. Dong, *Agronomy*, 2020, **10**, 746.
70 N. Xu, G. Tan, H. Wang and X. Gai, *Eur. J. Soil Biol.*, 2016, **74**, 1–8.
71 C. L. Lauber, M. Hamady, R. Knight and N. Fierer, *Appl. Environ. Microbiol.*, 2009, **75**, 5111–5120.
72 Y. Sheng and L. Zhu, *Sci. Total Environ.*, 2018, **622–623**, 1391–1399.
73 W. H. Hartman, C. J. Richardson, R. Vilgalys and G. L. Bruland, *Proc. Natl. Acad. Sci.*, 2008, **105**, 17842–17847.
74 B. Shahzad, M. Tanveer, W. Hassan, A. N. Shah, S. A. Anjum, S. A. Cheema and I. Ali, *Plant Physiol. Biochem.*, 2016, **107**, 104–115.
75 G. K. Johnson, R. T. Grow and W. N. Hubbard, *J. Chem. Thermodyn.*, 1975, **7**, 781–786.
76 G. Weber, E. Sciora, J. Guichard, F. Bouyer, I. Bezverkhyy, J. Marcos Salazar, C. Dirand, F. Bernard, H. Lecoq, R. Besnard and J.-P. Bellat, *J. Therm. Anal. Calorim.*, 2018, **132**, 1055–1064.
77 T. Ben-Moshe, S. Frenk, I. Dror, D. Minz and B. Berkowitz, *Chemosphere*, 2013, **90**, 640–646.
78 A. M. Kielak, C. C. Barreto, G. A. Kowalchuk, J. A. van Veen and E. E. Kuramae, *Front. Microbiol*, 2016, **7**, 744.
79 I. Hashmi, S. Bindschedler and P. Junier, in *Beneficial Microbes in Agro-Ecology*, ed. N. Amaresan, M. Senthil Kumar, K. Annapurna, K. Kumar and A. Sankaranarayanan, Academic Press, 2020, pp. 363–396, DOI: **10.1016/B978-0-12-823414-3.00018-6**.
80 C. Shen, Y. Ge, T. Yang and H. Chu, *J. Soils Sediments*, 2017, **17**, 2449–2456.
81 F. Thomas, J.-H. Hehemann, E. Rebuffet, M. Czjzek and G. Michel, *Front. Microbiol*, 2011, **2**, 00093.
82 K. Kersters, P. De Vos, M. Gillis, J. Swings, P. Vandamme and E. Stackebrandt, in *The Prokaryotes. Proteobacteria: Alpha and Beta Subclasses*, ed. M. Dworkin, S. Falkow, E. Rosenberg, K.-H. Schleifer and E. Stackebrandt, Springer New York, New York, NY, 2006, vol. 5, pp. 3–37.
83 S. Goldberg, H. S. Forster and C. L. Godfrey, *Soil Sci. Soc. Am. J.*, 1996, **60**, 425–432.
84 Z. Shi, E. Peltier and D. L. Sparks, *Environ. Sci. Technol.*, 2012, **46**, 2212–2219.

85 X. Wang, X. Li, F. Dou, W. Sun, K. Chen, Y. Wen and X. Ma, *Environ. Pollut.*, 2021, **290**, 118005.
86 W. Du, Y. Sun, R. Ji, J. Zhu, J. Wu and H. Guo, *J. Environ. Monit.*, 2011, **13**, 822–828.
87 H. Sekiguchi, N. Tomioka, T. Nakahara and H. Uchiyama, *Biotechnol. Lett.*, 2001, **23**, 1205–1208.
88 J. L. Kirk, L. A. Beaudette, M. Hart, P. Moutoglis, J. N. Klironomos, H. Lee and J. T. Trevors, *J. Microbiol. Methods*, 2004, **58**, 169–188.
89 K. Smalla, M. Oros-Sichler, A. Milling, H. Heuer, S. Baumgarte, R. Becker, G. Neuber, S. Kropf, A. Ulrich and C. C. Tebbe, *J. Microbiol. Methods*, 2007, **69**, 470–479.